Improving the speed of the genetic toggle switch without sacrificing its dynamic stability

Jiunn R. Chen*
Department of Molecular and Cellular Biology, Harvard University, Cambridge, Massachusetts, USA
(Received 7 October 2005; revised manuscript received 11 January 2006; published 3 April 2006)

Determinants of the switching speed of the genetic toggle switch remain unknown. Analysis shows that the decay rate of proteins predominantly sets the speed limit, but its modification introduces a trade-off between increased speed and decreased bistability. Incorporating protein-modifying enzymes into the switch gives extra degrees of freedom to address this trade-off. The condition for bistability when such enzymes are incorporated is derived. Under this condition, speed increases with the maximal rate of gene expression.

DOI: 10.1103/PhysRevE.73.041901 PACS number(s): 87.17.−d

There is increasing interest in applying tools from nonlinear dynamics to the design of synthetic genetic modules [1–4]. Here we analyze a prototype module, the genetic toggle switch. A common design [[5–7], see Fig. 1(a)] of the switch consists of two genes α and β. Gene α encodes repressor A, and its promoter Pr-α is inhibited by repressor B. Gene β encodes repressor B, and its promoter Pr-β is inhibited by repressor A. If the properties of the two genes are adjusted appropriately (such as the strength of promoters, the decay rate of proteins, the copy number of genes, etc.), the system will exhibit bistability: either gene α is active and gene β is inactive, or vice versa. This system can be externally controlled by applying drugs. To toggle the switch from one state to the other, one adds the inhibitor to the repressor of the suppressed gene, thereby relieving the gene from suppression and pushing the system towards an interstate unstable situation (the "saddle") [see Fig. 1(b)]. If pushed far enough, the system will move from there to the new state; otherwise, it will move back to the old state. One major challenge for the design of the switch is to increase its speed. Without theoretical guidance, the traditional "tinkering" approach of molecular biology is difficult, since there are too many parameters to adjust. Experimentally one would like the system to leave the saddle point as fast as possible once it is pushed thereto. Speed around the saddle point is therefore an important consideration, and we now turn to its analysis.

For simplicity, we assume the system is symmetric, i.e., the two genes share identical properties. They have the same gene expression rate, the same protein decay rate, etc. (In general, the more asymmetric the system is, the less likely the bistability property persists.)

The system's dynamics is described by the Hill model [5–8]

$$\partial_t X = \varepsilon/(1+\gamma Y^\kappa) - \eta X,$$

$$\partial_t Y = \varepsilon/(1+\gamma X^\kappa) - \eta Y, \qquad (1)$$

where X (UL^{-1}) and Y (UL^{-1}) represent the concentrations of the two repressors A and B, respectively, ε (UL^{-1} h^{-1}) is the maximal gene expression rate, $\gamma(U^{-\kappa}L^\kappa)$ is a coefficient governing the strength of repressors on gene expression, η (h^{-1}) is the decay rate of the repressors, and κ (unitless) is the Hill coefficient governing whether the repression is cooperative (in which case $\kappa>1$) or not (in which case $\kappa=1$). U is the unit of quantity for proteins; in many genetic systems, a suitable choice of U is nmole. L is liter, and h is hour. Previous studies have shown that the system has bistability only when $\kappa>1$ [5,6].

The two nullclines, $\partial_t X=0$ and $\partial_t Y=0$, in general intersect at three fixed points [5,6]. The middle fixed point is a saddle point, where $X=Y=\omega$ and $\eta\omega(1+\gamma\omega^\kappa)=\varepsilon$ due to the symmetry of the system. Near the saddle point the system is undergoing two orthogonal sets of flow [9], one being convergent towards the saddle point, the other divergent away from the saddle point and towards (one of) the stable states [Fig. 1(b)]. The time constants of these orthogonal flows are the inverse of the eigenvalues of the matrix [9]

$$\begin{pmatrix} -\eta & -\varepsilon\gamma\kappa\omega^{\kappa-1}/(1+\gamma\omega^\kappa)^2 \\ -\varepsilon\gamma\kappa\omega^{\kappa-1}/(1+\gamma\omega^\kappa)^2 & -\eta \end{pmatrix},$$

which are $\eta\{-1\pm\kappa[1-1/(1+\gamma\omega^\kappa)]\}$. The maximum value for the positive eigenvalue is $\eta(\kappa-1)$, and the minimum value for the negative eigenvalue is $-\eta(\kappa+1)$. The two eigenvalues approach these extremes when ω is large, or when ε/η is large, since $\omega<\varepsilon/\eta$.

This implies several things about the properties of the system. Firstly, the speed around the saddle point is predominantly limited by the decay rate of repressors (up to a multiplicative factor $\kappa\pm1$), irrespective of the strength of repression or the maximal rate of gene expression. Therefore, when speed is of concern, the decay rate of the repressors is the most important factor to consider [see Fig. 1(c)]. Secondly, attraction towards the saddle point is faster than the orthogonal repulsion from the saddle point [Fig. 1(b)]. Thirdly, the more the repressor functions cooperatively (the larger κ is), the faster the system becomes.

There is a limit to how fast one can engineer a protein to make it decay faster, and it is even more difficult to adjust the Hill coefficient κ of the repressors. Moreover, making the protein decay faster will, in general, abolish the bistability. Defining the "bistability index" of the system as the ratio between the concentration of a repressor at its "on" state and

*Mailing address: 34A Irving Street, #4, Cambridge, Massachusetts, 02138, USA. Email address: jrchen@fas.harvard.edu

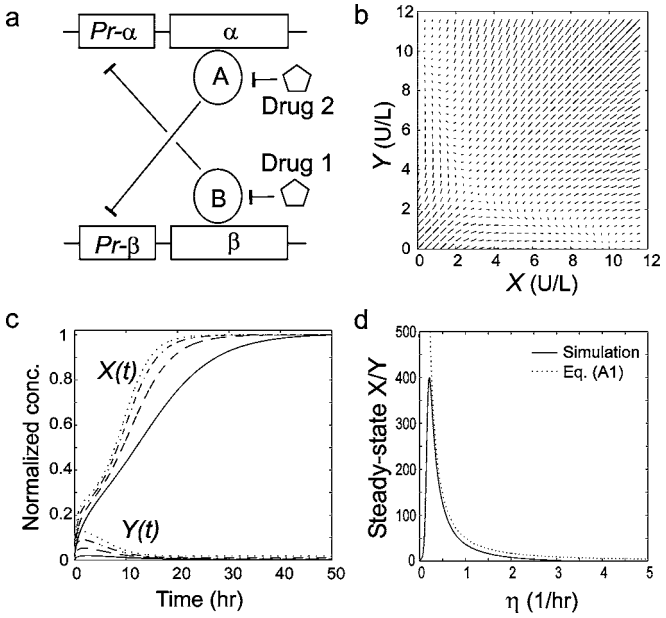

FIG. 1. Trade-off between speed and bistability in the genetic toggle switch. (a) Common design of the genetic toggle switch ([5–7]). (b) Flow field in the phase plane of the genetic toggle switch. Magnitude of speed is indicated by the length of marks. (c) Speed of the system increases as η increases. Simulation was done with the following parameters: $X(0)=2.0\%$ of the maximal level, $Y(0)=1.0\%$ of the maximal level, $\varepsilon=5.0$, $\gamma=5.0$, $\kappa=1.5$, and $\eta=0.2$ (—), 0.4 (– – –), 0.6 (–·–), 0.8 (···). Time step $\Delta t=0.005$. Both $X(t)$ and $Y(t)$ were normalized by their maximal levels. (d) The system loses bistability as the decay rate of the repressors η increases. Shown is the ratio between the steady-state concentrations of the two repressors as a function of η (system parameters: $\varepsilon=5.0$, $\gamma=5.0$, $\kappa=1.5$). Dotted line (···) is the approximation given by Eq. (A1).

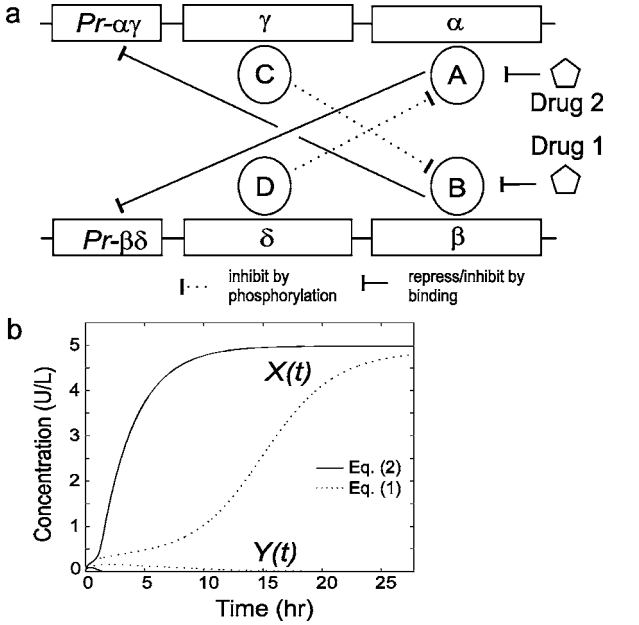

FIG. 2. Incorporation of protein-modifying enzymes into the toggle switch. (a) Topology of the system described by Eq. (2). (b) Speed of the system increases when enzymes are incorporated. Solid lines (—) represent the system described by Eq. (2) [simulation parameters: $X(0)=0.2$, $Y(0)=0.1$, $Z(0)=0$, $W(0)=0$, $\varepsilon=5.0$, $\gamma=5.0$, $\kappa=1.5$, $\eta=1.0$, $\lambda=2.0$, $K_m=2.0$, $\Delta t=0.005$]. Dotted lines (···) represent the system described by Eq. (1) (simulation parameters same as above, except $\lambda=0$ to account for the lack of enzymatic action).

that at its "off" state, the leading-order approximation of this ratio is $[1+\gamma(\varepsilon/\eta)^{\kappa}]/\{1+\gamma(\varepsilon/\eta)^{\kappa}[1+\gamma(\varepsilon/\eta)^{\kappa}]^{-\kappa}\}$ (see Appendix A) and approaches 1 as $\varepsilon/\eta\to 0$. This implies that the two stable states collapse into one when the protein decay rate is too fast [Fig. 1(d)]. Therefore, there is a trade-off between the operational speed and the maintenance of the bistability property, a result consistent with experimental observations [13].

However, it is not necessary to be constrained by the decay rate of proteins, as long as one can inhibit the function of the repressor through other methods. For example, often times chemical modification of the protein (e.g., phosphorylation) is faster than protein decay by several orders of magnitude, and one can take advantage of this high speed. A possible design of the toggle switch is shown in Fig. 2(a). Two kinase genes γ and δ are incorporated in the switch and driven by the same promoters as the repressor genes. Each kinase phosophorylates and inhibits one of the repressors. Simulation validates that this module can operate much faster than the system described by Eq. (1) [Fig. 2(b)].

To simplify the analysis, we assume the design is also symmetric. Its dynamics can be modeled by the following equations [5–8]:

$$\partial_t X = \varepsilon/(1+\gamma Y^{\kappa}) - \eta X - \lambda W X/(K_m + X),$$

$$\partial_t Y = \varepsilon/(1+\gamma X^{\kappa}) - \eta Y - \lambda Z Y/(K_m + Y),$$

$$\partial_t Z = \varepsilon/(1+\gamma Y^{\kappa}) - \eta Z,$$

$$\partial_t W = \varepsilon/(1+\gamma X^{\kappa}) - \eta W, \qquad (2)$$

where X, Y, ϵ, η, κ (>1) are defined as in Eq. (1) (for simplicity, all the protein species are assumed to have the same decay rate), Z (UL^{-1}) and W (UL^{-1}) are the concentrations of kinases C and D, respectively, λ (h^{-1}) is the rate constant of enzymatic action, and K_m (UL^{-1}) is the Michaelis constant.

The bistability index of the switch described by Eq. (2) is larger than that of the switch described by Eq. (1) (Appendix B and Fig. 3). As for the saddle point, X and Y are $\approx \eta K_m/\lambda$ when the maximal rate of gene expression ε is sufficiently large (Appendix C). The bifurcation diagram [Fig. 3] shows that the saddle point transforms into a stable fixed point (and the system no longer behaves as a toggle switch), when λ is too large. On the other hand, when λ is smaller than $\approx(\kappa\gamma)^{1/\kappa}K_m\eta$, the system has bistability, and the switching speed increases as ε increases (Appendix D). Increasing ε also increases the robustness against noise around the saddle point (Appendix E). It might seem counterintuitive that as λ increases, the system loses its bistability, since a larger λ implies a stronger mutual suppression through enzymatic action. The reason lies in the fact that enzymes, unlike repressors, are not consumed stoichiometrically during their action.

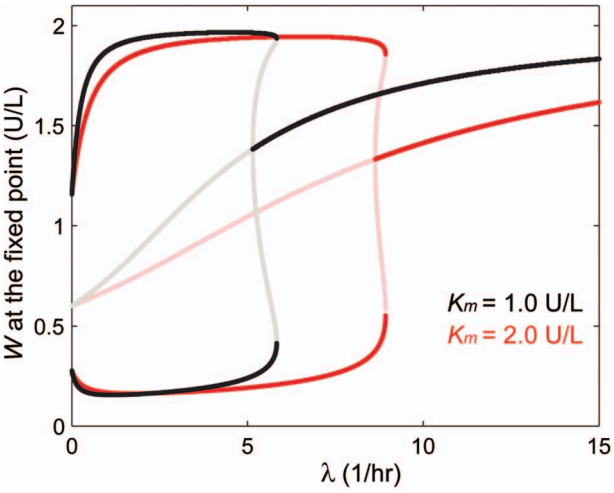

FIG. 3. (Color) Bifurcation diagram for the parameter λ. As λ increases from zero, the system first transforms from bistability into tristability, and then into monostability. Theoretical prediction for the boundary between bistability and its breakdown [Eq. (D1)] is $\lambda=3.8$ when $K_m=1.0$, and $\lambda=7.7$ when $K_m=2.0$. Increasing K_m expands the territory of bistability. Values of other parameters: $\varepsilon=2.0$, $\gamma=5.0$, $\kappa=1.5$, and $\eta=1.0$. Unstable branches are drawn in light colors, and stable branches in dark. Note that $\lambda=0$ corresponds to the system described by Eq. (1).

When λ is too large, even at its "off-state," low concentration, the enzyme is able to inhibit most of the repressors of its encoding gene.

So far we have been assuming our systems are symmetric [Eqs. (1) and (2)]. What would happen if this symmetry were broken? It has been shown [5] that the system described by Eq. (1) is more tolerant of asymmetry in ε if the Hill coefficient κ is larger. A similar argument can be made regarding λ and K_m in the system described by Eq. (2) (Appendix F). In practice, it is difficult to find a pair of enzymes with identical parameters, but as long as λ_1/λ_2 is on the order of K_{m1}/K_{m2}, the system can have bistability [Fig. 4(a)]. Moreover, tolerance towards asymmetry in enzyme parameters λ and K_m increases with the maximal gene expression rate ε, the strength of repressors γ, and the Hill coefficient of repressors κ [Fig. 4(b)].

Previous studies have demonstrated the usefulness of theoretical analysis in the prediction of steady-state behavior of a synthetic gene network [4–6]. Here we investigated another equally important, but less studied, property of a gene network: its operational speed. Our case study of the toggle switch suggests that there is a trade-off between speed and bistability. This trade-off is mainly dictated by the decay rate of the protein function. We predict that incorporating protein-modifying enzymes would help tackle this trade-off. Repressor-inhibiting enzymes are not uncommon in nature. To give several examples: the mammalian protein kinase *C* phosphorylates and inhibits *p*97, a repressor of aldolase *A* *L*-type promoter [10]; the yeast cyclin-dependent kinase phosphorylates Whi5, dissociating it from SBF and relieving the repression of G1/S transcription [11]; and the mammalian cAMP-dependent protein kinase phosphorylates and decreases the DNA-binding ability of the product of the Wilms' tumor suppressor gene (WT1) [12]. These enzymes could be incorporated into future designs of the toggle switch.

J.R.C. thanks M.P. Brenner, J.J. Collins, T.S. Gardner, G.B. Stanley, and Y.H. Sun for invaluable discussions. J.R.C. is supported in part by an N.I.H. training grant in Genetics and Genomics.

APPENDIX A

Without loss of generality, we assume the system described by Eq. (1) [see Fig. 1(a)] is currently in one of the stable states such that $X \gg Y$. It can be shown that $X \approx \varepsilon/\eta\{1+\gamma(\varepsilon/\eta)^{\kappa}[1+\gamma(\varepsilon/\eta)^{\kappa}]^{-\kappa}\}$ and $Y \approx \varepsilon/\eta[1+\gamma(\varepsilon/\eta)^{\kappa}]$. The bistability index is the ratio

$$X/Y \approx [1+\gamma(\varepsilon/\eta)^{\kappa}]/\{1+\gamma(\varepsilon/\eta)^{\kappa}[1+\gamma(\varepsilon/\eta)^{\kappa}]^{-\kappa}\}. \tag{A1}$$

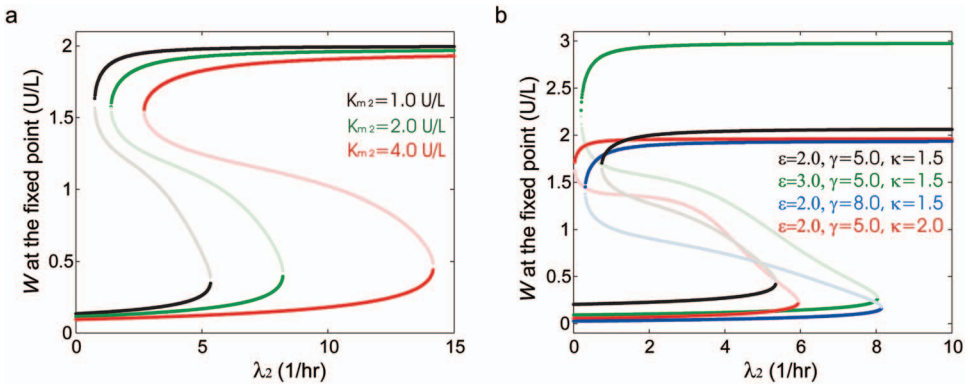

FIG. 4. (Color) (a) Bifurcation diagram for the parameter λ_2 at different values of K_{m2}. Values of other parameters: $\varepsilon=2.0$, $\gamma=5.0$, $\kappa=1.5$, $\eta=1.0$, $K_{m1}=1.0$, and $\lambda_1=3.0$. (b) Bifurcation diagram for the parameter λ_2 at different values of ε, γ, and κ. Values of other parameters: $\eta=1.0$, $K_{m1}=K_{m2}=1.0$, and $\lambda_1=3.0$. Unstable branches are drawn in light colors, and stable branches in dark. Plots of different colors are slightly vertically translated to prevent superposition. See Appendix F for the mathematical details.

APPENDIX B

Without loss of generality, we assume the system described by Eq. (2) [see Fig. 2(a)] is currently in one of the stable states such that $X,Z \gg Y,W$. It can be shown that

$$X \approx \varepsilon/\eta\{1+\varepsilon\lambda/\eta^2[1+\gamma(\varepsilon/\eta)^\kappa](K_m+\varepsilon/\eta)\},$$

$$Y \approx \varepsilon/\eta(1+\lambda\varepsilon/\eta^2 K_m)[1+\gamma(\varepsilon/\eta)^\kappa],$$

$$Z \approx \varepsilon/\eta\{1+\gamma(\varepsilon/\eta)^\kappa[1+\gamma(\varepsilon/\eta)^\kappa]^{-\kappa}(1+\lambda\varepsilon/\eta^2 K_m)^{-\kappa}\},$$

and

$$W \approx \varepsilon/\eta[1+\gamma(\varepsilon/\eta)^\kappa].$$

The bistability index is the ratio Z/W, which is the product of the bistability index of the system described by Eq. (1) [Eq. (A1)] and $Q \equiv \{1+\gamma(\varepsilon/\eta)^\kappa[1+\gamma(\varepsilon/\eta)^\kappa]^{-\kappa}\}/\{1+\gamma(\varepsilon/\eta)^\kappa[1+\gamma(\varepsilon/\eta)^\kappa]^{-\kappa}(1+\lambda\varepsilon/\eta^2 K_m)^{-\kappa}\}$. Note that $Q>1$.

APPENDIX C

By symmetry arguments, at the saddle point $X=Y=\theta$, $Z=W=\omega$, $0=\partial_t X=\partial_t Y=\varepsilon/(1+\gamma\theta^\kappa)-\eta\theta-\lambda\theta\omega/(K_m+\theta)$, and $0=\partial_t Z=\partial_t W=\varepsilon/(1+\gamma\theta^\kappa)-\eta\omega$. The last two equations can be combined into one:

$$0=\varepsilon[1-\lambda\theta/\eta(K_m+\theta)]-\eta\theta(1+\gamma\theta^\kappa). \tag{C1}$$

Defining $f(\theta)\equiv\varepsilon[1-\lambda\theta/\eta(K_m+\theta)]-\eta\theta(1+\gamma\theta^\kappa)$, $f(0)=\varepsilon>0$, $f(\infty)=-\infty<0$, and $f(\theta)$ is a strictly monotonously decreasing function when $\theta>0$. Therefore, there must be a unique positive real-number solution for θ satisfying Eq. (C1), and it is easy to see that $\theta\to 0$ as $\lambda\to\infty$. Solving the leading-order approximation of θ when λ is large, we get $\theta\approx\eta K_m/\lambda$. This approximation remains valid when $\varepsilon \gg \eta^2 K_m/\lambda$.

APPENDIX D

Around the fixed point $(X,Y,Z,W)=(\theta,\theta,\omega,\omega)$,

$$\partial_t\begin{pmatrix} X-\theta \\ Y-\theta \\ Z-\omega \\ W-\omega \end{pmatrix} = M\begin{pmatrix} X-\theta \\ Y-\theta \\ Z-\omega \\ W-\omega \end{pmatrix},$$

where

$$M=\begin{pmatrix} -\eta-\Sigma & -\Omega & 0 & -\Psi \\ -\Omega & -\eta-\Sigma & -\Psi & 0 \\ 0 & -\Omega & -\eta & 0 \\ -\Omega & 0 & 0 & -\eta \end{pmatrix},$$

$$\Sigma=\varepsilon\lambda K_m/\eta(K_m+\theta)^2(1+\gamma\theta^\kappa),$$

$\Omega=\varepsilon\gamma\kappa\theta^{\kappa-1}/(1+\gamma\theta^\kappa)^2$, and $\Psi=\lambda\theta/(K_m+\theta)$.

Denoting

$$p=[\Sigma+\Omega+\sqrt{(\Sigma+\Omega)^2+4\Omega\Psi}]/2\Omega,$$

$$q=-[\Sigma+\Omega-\sqrt{(\Sigma+\Omega)^2+4\Omega\Psi}]/2\Omega,$$

$$s=[-\Sigma+\Omega+\sqrt{(-\Sigma+\Omega)^2+4\Omega\Psi}]/2\Omega,$$

and

$$t=-[-\Sigma+\Omega-\sqrt{(-\Sigma+\Omega)^2+4\Omega\Psi}]/2\Omega,$$

the (normalized) eigenvectors of M are $(p,p,1,1)^T/\sqrt{2(1+p^2)}$, $(-q,-q,1,1)^T/\sqrt{2(1+q^2)}$, $(s,-s,1,-1)^T/\sqrt{2(1+s^2)}$, and $(-t,t,1,-1)^T/\sqrt{2(1+t^2)}$, and their respective eigenvalues are $-\eta-p\Omega$, $-\eta+q\Omega$, $-\eta+s\Omega$, and $-\eta-t\Omega$, respectively. Note $p,q,s,t>0$.

The eigenvector $(s,-s,1,-1)^T/\sqrt{2(1+s^2)}$, is parallel to the axis of toggle switching, and therefore its associated eigenvalue $-\eta+s\Omega$ has to be positive. If ε is sufficiently large, it can be shown that $\lambda<\lambda_{u.b.}$, where

$$\lambda_{u.b.} \equiv (\kappa\gamma)^{1/\kappa}K_m\eta \tag{D1}$$

guarantees $\Omega<\Sigma$, and the eigenvalue $-\eta+s\Omega$ is greater than $-\eta+\sqrt{\Omega\Psi}>-\eta+\sqrt{\varepsilon\lambda/K_m(1+\eta/\lambda)[1+\gamma(K_m\eta/\lambda)^\kappa]^2}$, which is always positive if $\varepsilon>(\eta^2K_m/\lambda)(1+\eta/\lambda)[1+\gamma(K_m\eta/\lambda)^\kappa]^2$. Under this condition, the eigenvalue grows with ε at least as fast as $-\eta+\sqrt{\varepsilon\lambda/K_m(1+\eta/\lambda)[1+\gamma(K_m\eta/\lambda)^\kappa]^2}$. Note that $\lambda_{u.b.}$ is not a tight upper bound for λ.

APPENDIX E

We now study the effect of noise on the behavior of the system described by Eq. (2) around the saddle point,

$$\partial_t\begin{pmatrix} X-\theta \\ Y-\theta \\ Z-\omega \\ W-\omega \end{pmatrix} = M\begin{pmatrix} X-\theta \\ Y-\theta \\ Z-\omega \\ W-\omega \end{pmatrix} + \begin{pmatrix} \xi_1 \\ \xi_2 \\ \xi_3 \\ \xi_4 \end{pmatrix},$$

where ξ_i's are four independent stochastic processes with zero mean and $\langle\xi_i(t)\xi_i(t')\rangle=\sigma^2\delta(t-t')$, $\forall i\in\{1,2,3,4\}$. $\delta(\cdot)$ is Dirac's delta function.

According to Appendix D, the evolution of the system along the axis of toggle switching $\psi\equiv[s(X-Y)+Z-W]/\sqrt{2(1+s^2)}$ is described by

$$\partial_t\psi=\varsigma\psi+\rho, \tag{E1}$$

where $\varsigma=-\eta+s\Omega>0$ is the eigenvalue of the matrix M for the eigenvector $(s,-s,1,-1)^T/\sqrt{2(1+s^2)}$, and $\rho=[s(\xi_1-\xi_2)+\xi_3-\xi_4]/\sqrt{2(1+s^2)}$ is a stochastic process with zero mean and $\langle\rho(t)\rho(t')\rangle=\sigma^2\delta(t-t')$.

Eq. (E1) can be solved to give

$$\psi(t)=\exp(\varsigma t)\psi(0)+\Gamma(t), \tag{E2}$$

where $\Gamma(t)=\int_0^t dt'\exp[\varsigma(t-t')]\rho(t')$ is a stochastic process with zero mean. The variance of $\Gamma(t)$ is given by

$$\langle(\Gamma(t))^2\rangle=\left\langle \int_0^t dt' \exp[\varsigma(t-t')]\rho(t') \int_0^t dt'' \exp[\varsigma(t-t'')]\rho(t'') \right\rangle=\left\langle \int_0^t dt' \exp[\varsigma(t-t')] \int_0^t dt'' \exp[\varsigma(t-t'')]\rho(t')\rho(t'') \right\rangle.$$

$$=\int_0^t dt' \exp[\varsigma(t-t')] \int_0^t dt'' \exp[\varsigma(t-t'')]\langle\rho(t')\langle\rho(t'')\rangle=\int_0^t dt' \exp[\varsigma(t-t')] \int_0^t dt'' \exp[\varsigma(t-t'')]\sigma^2\delta(t'-t'')=(\sigma^2/2\varsigma)$$

$$\times[\exp(2\varsigma t)-1].$$

Therefore, $|\Gamma(t)|$ is on the order of $\sqrt{(\sigma^2/2\varsigma)[\exp(2\varsigma t)-1]}$. If $\sigma^2/2\varsigma$ is small, the term $\exp(\varsigma t)\psi(0)$ dominates in Eq. (E2), and the system's evolution is determined by the initial condition $\psi(0)$. On the other hand, if $\sigma^2/2\varsigma$ is large, eventually the noise term $\Gamma(t)$ dominates, and there is a chance that the system will move in the wrong direction.

As shown in Appendix D, ς grows with the maximal rate of gene expression ε at least as fast as $-\eta+\sqrt{\varepsilon\lambda/K_m(1+\eta/\lambda)[1+\gamma(K_m\eta/\lambda)^\kappa]^2}$. Thus, it is possible to increase the robustness against noise by increasing the maximal gene expression rate.

An equation similar to Eq. (E1) can be derived for the system described by Eq. (1). In this case, the eigenvalue ς is always less than $\eta(k-1)$, and this ceiling determines the maximal magnitude of noise the system can tolerate.

APPENDIX F

We now model asymmetry in the system described by Eq. (2) as follows: Let λ_1 and λ_2 be the rate constants of kinases C and D, respectively, andK_{m1} and K_{m2} be their Michaelis constants. Equation (2) becomes

$$\partial_t X=\varepsilon/(1+\gamma Y^\kappa)-\eta X-\lambda_2 WX/(K_{m2}+X),$$

$$\partial_t Y=\varepsilon/(1+\gamma X^\kappa)-\eta Y-\lambda_1 ZY/(K_{m1}+Y),$$

$$\partial_t Z=\varepsilon/(1+\gamma Y^\kappa)-\eta Z,$$

$$\partial_t W=\varepsilon/(1+\gamma X^\kappa)-\eta W. \tag{F1}$$

Without loss of generality, we assume the system still has bistability and is currently in one of the stable states such that $X,Z\approx\varepsilon/\eta$ and $Y,W\approx 0$, then $0=\partial_t X<\varepsilon-\{\eta+\varepsilon\lambda_2/\eta[1+\gamma(\varepsilon/\eta)^\kappa](K_{m2}+\varepsilon/\eta)\}X$, or $X<\Lambda\equiv\varepsilon/\eta\{1+\varepsilon\lambda_2/\eta^2[1+\gamma(\varepsilon/\eta)^\kappa](K_{m2}+\varepsilon/\eta)\}$. On the other hand, we have $0=\partial_t Y\varepsilon>[1+\gamma(\varepsilon/\eta)^\kappa]-(\eta+\varepsilon\lambda_1/\eta K_{m1})Y$, or $Y>\Lambda'\equiv\varepsilon/\eta[1+\gamma(\varepsilon/\eta)^\kappa](1+\varepsilon\lambda_1/\eta^2K_{m1})$. Obviously, Λ has to be much larger than Λ',or

$$1+\varepsilon\lambda_2/\eta^2[1+\gamma(\varepsilon/\eta)^\kappa](K_{m2}+\varepsilon/\eta) \ll[1+\gamma(\varepsilon/\eta)^\kappa](1+\varepsilon\lambda_1/\eta^2K_{m1}). \tag{F2}$$

Similarly, we have

$$1+\varepsilon\lambda_2/\eta^2[1+\gamma(\varepsilon/\eta)^\kappa](K_{m1}+\varepsilon/\eta) \ll[1+\gamma(\varepsilon/\eta)^\kappa](1+\varepsilon\lambda_2/\eta^2K_{m2}). \tag{F3}$$

It can be shown that

$$[1+\gamma(\varepsilon/\eta)^\kappa]^{-2}\ll(\lambda_1/\lambda_2)/(K_{m1}/K_{m2})\ll[1+\gamma(\varepsilon/\eta)^\kappa]^2 \tag{F4}$$

guarantees both Eqs. (F2) and (F3) are satisfied. While Eq. (F4) is not a sufficient condition for bistability, it does suggest that λ_1/λ_2 has to scale with K_{m1}/K_{m2}. Equation (F4) also predicts that tolerance towards asymmetry increases with ε, γ, and κ.

[1] J. Hasty, D. McMillen, and J. J. Collins, Nature (London) **420**, 224 (2002).

[2] M. Kaern, T. C. Elston, W. J. Blake, and J. J. Collins, Nat. Rev. Genet. **6**, 451 (2005).

[3] S. A. Benner and A. M. Sismour, Nat. Rev. Genet. **6**, 533 (2005).

[4] J. Hasty, M. Dolnik, V. Rottschäfer, and J. J. Collins, Phys. Rev. Lett. **88**, 148101 (2002).

[5] T. S. Gardner, C. R. Cantor, and J. J. Collins, Nature (London) **403**, 339 (2000).

[6] T. S. Gardner, Ph.D. thesis, Boston University 2000 (unpublished).

[7] B. P. Kramer, A. U. Viretta, M. Daoud-El-Baba, D. Aubel, W. Weber, and M. Fussenegger, Nat. Biotechnol. **22**, 867 (2004).

[8] L. Stryer, *Biochemistry* (Freeman, New York, 1995).

[9] S. H. Strogatz, *Nonlinear Dynamics and Chaos: With Applications to Physics, Biology, Chemistry and Engineering* (Perseus, Cambridge, 1994).

[10] P. Costanzo, A. Lupo, P. D'Agostino, C. Zevino, and P. Izzo, FEBS Lett. **454**, 61 (1999).

[11] M. Costanzo, J. L. Nishikawa, X. Tang, J. S. Millman, O. Schub, K. Breitkreuz, D. Dewar, I. Rupes, B. Andrews, and M. Tyers, Cell **117**, 899 (2004).

[12] Y. Sakamoto, M. Yoshida, K. Semba, and T. Hunter, Oncogene **15**, 2001 (1997).

[13] T. S. Gardner and J. J. Collins (private communication).